

Fluorescent dissolved organic matter as a multivariate biogeochemical tracer of submarine groundwater discharge in coral reef ecosystems

Craig E. Nelson^{a,*}, Megan J. Donahue^b, Henrieta Dulaiova^c, Stuart J. Goldberg^a, Florybeth F. La Valle^b, Katie Lubarsky^b, Justin Miyano^b, Christina Richardson^c, Nyssa J. Silbiger^b, Florence I.M. Thomas^b

^a Center for Microbial Oceanography: Research and Education, Department of Oceanography and Sea Grant College Program, School of Ocean and Earth Science and Technology, University of Hawai'i at Mānoa, Honolulu, HI 96822, USA

^b Hawai'i Institute of Marine Biology, School of Ocean and Earth Science and Technology, University of Hawai'i at Mānoa, Honolulu, HI 96822, USA

^c Department of Geology and Geophysics, School of Ocean and Earth Science and Technology, University of Hawai'i at Mānoa, Honolulu, HI 96822, USA

ARTICLE INFO

Article history:

Received 11 March 2015

Received in revised form 25 June 2015

Accepted 26 June 2015

Available online 3 July 2015

Keywords:

Dissolved organic matter

Groundwater

Coral reefs

Islands

ABSTRACT

In Hawai'i and other Pacific high islands submarine groundwater discharge (SGD) can be a significant and continuous source of solutes to nearshore reefs and may play a key role in the structure and function of benthic coral and algal communities. Identifying SGD sources and linking them to reef biogeochemistry is technically challenging. Here we analyzed spectra of fluorescent dissolved organic matter (fDOM) in coral reefs in the context of a suite of biogeochemical parameters along gradients of SGD to characterize fDOM composition and evaluate the utility of fDOM signatures in tracking groundwater dispersal and transformation. We spatially mapped water column chemistry in Maunalua Bay, Oahu, Hawai'i by collecting 24 water samples in grids at each of two ~0.15 km² regions during both high and low tides over a two-day period. We observed clear horizontal gradients in the majority of 15 measured parameters, including inorganic and organic solutes and organic particles that tracked concentrations of conservative SGD tracers (radon, salinity and silicate). Multivariate scanning excitation–emission fluorometry successfully differentiated two distinct groundwater sources and delineated regions of SGD dispersion in each reef from the surrounding water column samples without detectable groundwater. Groundwater was consistently depleted in DOC and enriched in nutrients; although the two SGD sources varied widely in fDOM quantity and fluorophore proportions, indices of humification were consistently elevated in SGD at both sites. Our results provide a robust spectral characterization of fDOM in SGD-influenced coral reefs and indicate the potential for this rapid and cost-effective measurement technique to be useful in tracking SGD dispersal in nearshore ecosystems.

© 2015 Elsevier B.V. All rights reserved.

1. Introduction

Coastal ecosystems experience dynamic inputs of material from benthic, fluvial, groundwater and offshore habitats. Groundwater can be a significant and continuous source of solutes to nearshore reefs and may play a key role in the structure and function of benthic coral and macroalgal communities, as well as influencing local coastal oceanography and planktonic communities. Groundwater nutrient and organic matter pollution, whether through agricultural fertilization, on-site sewage disposal, or runoff from industrial/urban land uses, is a major eutrophication concern for coral reefs because of reef adaptation to relatively low nutrient conditions (Fabricius, 2005; Lapointe, 1997). However, identifying groundwater sources and linking them to reef biogeochemistry is technically challenging.

Coral reefs are highly productive ecosystems adapted to oligotrophic oceans, and it remains an open question how they acquire sufficient

macro- and micro-nutrients to maintain high productivity in low-nutrient waters (e.g., Alldredge et al., 2013). Submarine groundwater discharge (SGD) is a phenomenon common to the Hawaiian Islands (Dollar and Atkinson, 1992; Johnson et al., 2008; Street et al., 2008; Swarzenski et al., 2013) and other Pacific high islands (Kim et al., 2011) wherein groundwater is continuously and directly discharged into shallow coastal reef ecosystems. SGD is assumed to be a fundamental feature of reef ecosystems where fluxes are significant (Cyronak et al., 2014; Paytan et al., 2006), and tracking the rate and extent of groundwater dispersion in coastal regions has been an area of significant active research in Hawai'i and elsewhere (Johnson et al., 2008; Knee et al., 2010; Moore, 2010; Street et al., 2008). Current techniques to understand where and when SGD is diffused throughout the nearshore habitat include thermal imaging (Johnson et al., 2008), dye tracer studies (Burnett et al., 2006), geophysical exploration (Dimova et al., 2012), radioisotopic tracers (Charette et al., 2008), and mapping of conservative solute concentrations (Street et al., 2008).

The influence of SGD on the structure and function of coral reefs is poorly understood. The elevated levels of nitrate and phosphate found

* Corresponding author.

E-mail address: craig.nelson@hawaii.edu (C.E. Nelson).

in SGD in many regions of Hawai'i (Johnson et al., 2008; Knee et al., 2010; Street et al., 2008) have been implicated as a key factor in coastal eutrophication (Dailer et al., 2010), changes in benthic algal composition (Smith et al., 2010; Stimson and Larned, 2000) and alteration of nearshore plankton biomass and community structure (Fabricius, 2005; McCook, 1999; Parsons et al., 2008). Despite our conceptualization of SGD as driving eutrophication, we have few studies mapping the distribution of organic matter in the water column of reefs experiencing significant SGD inputs (Tedetti et al., 2011). A key question for the role of SGD in coral ecosystems is how SGD may influence the organic composition of coral reefs, both through allochthonous subsidies and through stimulation of autochthonous productivity.

Dissolved organic matter (DOM) in aquatic ecosystems is a significant component of the total organic content of marine ecosystems. The pool of DOM in the oceans is vast, containing carbon equivalent to the CO₂ in the Earth's atmosphere, and compositionally complex, with degradation time scales that vary greatly from hours to many years (Hansell and Carlson, 2014). A portion of DOM fuels food webs through metabolism by single-celled osmotrophs such as heterotrophic Bacteria and Archaea that are subsequently grazed by microbial eukaryotes, a process known as the "microbial loop" (Azam et al., 1983). The organic matter content of groundwater can vary widely depending on the geological and hydrological factors defining groundwater catchments and biogeochemical processes altering solutes within the subterranean estuary (STE) (Kim et al., 2012). SGD in island systems can be sourced from a variety of different ages and levels of human impact (Knee et al., 2010; Wolanski et al., 2009), and little is known about the characteristics of groundwater organic matter in Pacific islands (Tedetti et al., 2011). SGD passes through the STE, a biogeochemical reactor that is analogous in metabolic complexity to surface estuaries where terrestrial freshwater and recirculated seawater mix, differing markedly with regards to sunlight exposure, residence time and redox conditions. The sources of DOM in the STE can be diverse and include terrestrial inputs (Tedetti et al., 2011), locally produced DOM within the STE (Santos et al., 2009), and marine DOM, which enters the STE via seawater recirculating through the coastal aquifer (Beck et al., 2007; Goñi and Gardner, 2003; Kim et al., 2012). Direct allochthonous DOM subsidies from SGD may have varying degrees of lability relative to ambient DOM depending on age and composition (Burdige et al., 2004; Kim et al., 2012); if allochthonous DOM in SGD is labile, it could stimulate the microbial loop in reefs thereby supporting a portion of the reef food web. Autochthonous production stimulated by SGD nutrient subsidies may also produce labile DOM that supports higher trophic levels (Johnson and Wiegner, 2013; Lee et al., 2010). Both subsidies of DOM may have significant impacts on reef ecosystem function, and understanding the relationship between SGD and DOM in reefs is an important step toward understanding how SGD influences reef ecosystems and how groundwater contamination may alter ecosystems processes.

The composition of DOM in aquatic environments is known to be highly complex, comprising a diverse suite of thousands of molecules ranging in molecular weight across many orders of magnitude (Hansell and Carlson, 2014). One method of characterizing DOM is through spectral analysis of a subset of DOM that exhibits autofluorescence, typically stimulated by ultraviolet and blue light (Coble, 1996). This fluorescent DOM (fDOM) can exhibit variable fluorescence across a range of excitation and emission wavelengths, and scanning fluorescence spectroscopy can produce a three dimensional map of the fDOM in a sample that varies through space and time according to subtle shifts in chemical composition of the complex molecular assemblage (Nelson and Coble, 2009). Analysis of the multivariate spectral characteristics of fDOM by generating an excitation–emission matrix (EEM) from a sample is a cost-effective analysis that requires minimal laboratory training and equipment and can produce a suite of informative data about the organic matter chemistry of the water. In marine ecosystems, the variation in fDOM characteristics has been used to differentiate between a variety of DOM sources including terrestrial (Coble, 1996), algal

(Determann et al., 1998), microbial (Stedmon and Markager, 2005) and anthropogenic (Dabestani and Ivanov, 1999; Ferretto et al., 2014). Additionally, fDOM characterization has proven useful in differentiating contributions from rivers, groundwater, coastal margins and reefs, and the open ocean (Chen et al., 2003; Helms et al., 2013; Osburn et al., 2013; Tedetti et al., 2011). If fDOM exhibits clearly defined characteristics across gradients of SGD influence it has the potential to serve as a promising tool for understanding the role of groundwater in reef ecosystems.

The present study sought to examine the relationship between SGD inputs and the field of particulate, dissolved and fluorescent organics in coral reef ecosystems. We identified two regions of a single contiguous reef system with relatively predictable nearshore inputs of SGD (Maunalua Bay, O'ahu, Hawai'i), which range from 12,000 to 16,000 m³ d^{−1} (Holleman, 2011). SGD here is composed of brackish groundwater (salinity of 2–5) discharging through channelized groundwater conduits (Dimova et al., 2012) thus bypassing STE processes typical for tidal flats. Since the water contains minimal recirculated seawater and an extensive STE is absent, its terrestrial DOM signature is preserved making it a unique SGD tracer. We first mapped the extent of SGD by collecting water samples in a grid centered on an identified spring discharge site at low and high tide and measuring a suite of inorganic solute concentrations, including relatively conservative groundwater tracers (salinity, radon and silicate) and various chemical species of N and P. From these same water samples we collected a suite of dissolved and particulate organic matter samples, including bulk measurements of DOM, particulate organic C and N, chlorophyll and cytometric counts of picoplankton and bacterioplankton. We tested whether these parameters correlated spatially and by site with the inorganic solutes measured, examining if samples from different regions of the reef clustered together in patterns consistent with SGD influence on the organic matter field. Finally, we conducted spectral analyses on fDOM to understand the characteristics of fDOM in different groundwater sources and evaluate the potential for tracking SGD dispersal and alteration across the reef ecosystem. Our results demonstrate that SGD in coral reef habitats alters not only the composition of inorganic solutes such as salinity, silicate and nutrients, but also bulk concentrations of dissolved and particulate organics and the spectral characteristics of fDOM. We discuss the potential for fDOM measurements to be developed into a cost-effective tool for tracking SGD in similar coral reefs dominated by spring groundwater inputs.

2. Methods

2.1. Water collection

We collected water samples at each of two nearshore fringing coral reef sites within Maunalua Bay, O'ahu, Hawai'i (Fig. 1a) over a two day period; 24 samples were collected near Waiupe Beach Park on 28 May 2014 and 24 samples were collected at Black Point on 29 May 2014 (Fig. 1b, c). The majority of samples (32 of 48) were collected synoptically during morning low tides (−6 to −9 cm) with an additional subset (16) collected during afternoon high tides (+67 cm; Fig. S1). Depths at these sites are generally <2 m, and the majority of samples (38) were collected from the surface (0.2 m below sea level); a subset of samples were additionally collected from bottom waters (roughly 0.2 m above the benthos). Using kayaks, surface water samples were hand-collected into 5 L high-density polyethylene carboys (73062, US Plastics, Lima, OH, USA); bottom water samples were collected in 5 L horizontal Niskin samplers (101005H, General Oceanics, Miami, FL, USA) and immediately siphoned to carboys for processing. Carboys and Niskin samplers were previously conditioned with seawater, soaked overnight in 10% HCl, thoroughly rinsed with low-organic deionized water (DIW; Barnstead Nanopure Diamond, Thermo Fisher Scientific, Asheville, NC, USA) and stored dry before sampling. All sample containers were also triple-rinsed with sample water before filling.

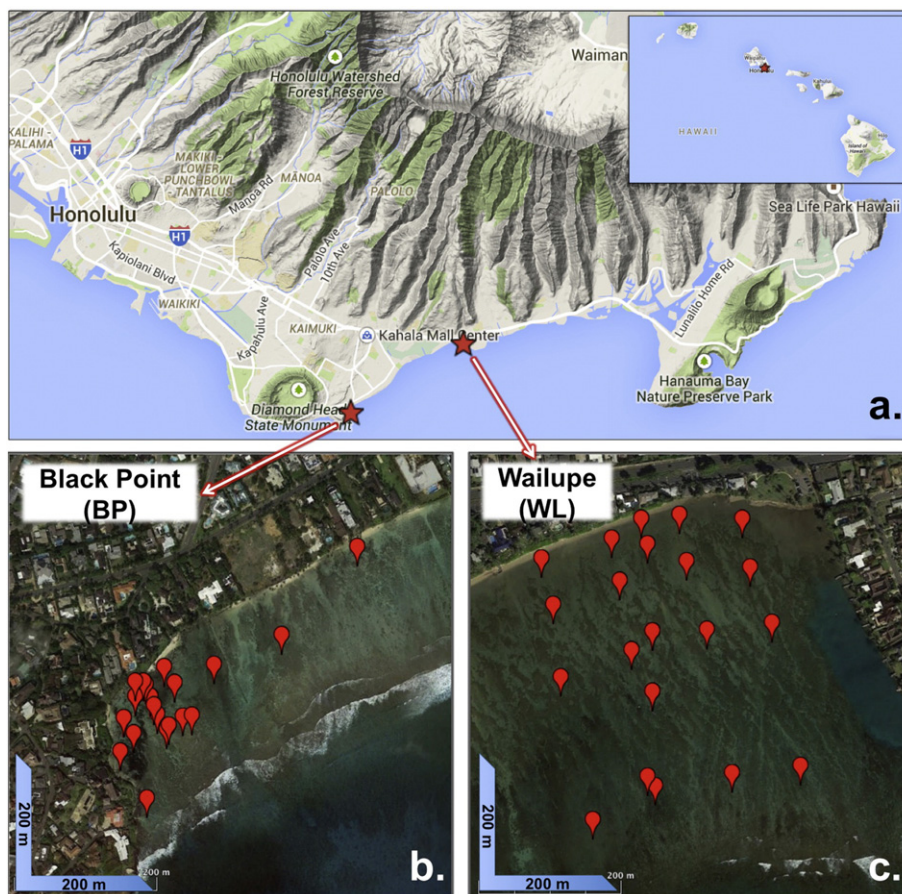


Fig. 1. Maps of the sampling locations. Panel a shows the location of the two sampling sites in Maunaloa Bay, Oahu, with the inset showing the location within the main Hawaiian islands. Water samples were collected at each site, Black Point to the West (b) and Wailupe to the East (c), with red markers at each location where water was collected.

All filtration and subsampling of water was done on site within 2 h of collection.

2.2. Sample collection and storage

All storage vials were acid soaked, thoroughly rinsed with DIW, air dried, and then triple rinsed with sample water before collection. Samples for total alkalinity (TA) were collected first directly from the carboy spigot. Duplicate TA samples (125 mL each) were transferred into polypropylene sample bottles (Huang et al., 2012) and amended with 50 μL of half-saturated HgCl_2 . All subsequent samples were transferred to long-term storage vials via gentle (1 mL s^{-1}) peristaltic pumping directly from the carboy through platinum-cured silicone tubing over a period of roughly 1 h. For dissolved nutrient analyses, the filtrate from a $0.2 \mu\text{m}$ polyethersulfone filter (Sterivex, Millipore, Billerica, MA, USA) was collected in acid-washed and sample rinsed 50 mL polypropylene tubes and frozen to -20°C . Samples for fDOM analysis were collected from the $0.2 \mu\text{m}$ polyethersulfone filtrate (after a minimum of 250 mL sample flushing to avoid filter DOM leaching) in amber glass vials with teflon-lined septate caps (acid-washed and DIW rinsed) and stored in a dark refrigerator free of volatile organics. For dissolved organic carbon (DOC) analyses the filtrate from glass fiber filters (Whatman GF/F, GE Life Sciences, Pittsburgh, PA, USA) was collected in glass vials with teflon-lined septate caps (acid-washed and DIW rinsed) and frozen to -20°C in an organic-free freezer. All glass vials and filters were pre-combusted within days of sampling (2 h at 400°C) and stored in a laboratory free of volatile organics. For analysis of chlorophyll *a* and particulate organic carbon/nitrogen, 600 to 1000 mL of sample water for each sample was filtered onto a 25 mm GF/F filter, folded in half,

wrapped in Al foil and frozen to -20°C . For flow cytometry (FCM), 1.5 mL of unfiltered water was fixed at 0.5% paraformaldehyde (amended with 100 μL 8% ampulated paraformaldehyde, Electron Microscopy Sciences, Hatfield, PA, USA) in a 2 mL polypropylene cryovial, mixed briefly and then frozen to -80°C . All samples were immediately refrigerated in the field and frozen or refrigerated within 6 h of collection for long-term storage.

2.3. Inorganic nutrient and organic matter concentration measurements

Nutrient samples were thawed to room temperature, mixed thoroughly and analyzed on a Seal Analytical Segmented Flow Injection AutoAnalyzer AA3HR for simultaneous determination of soluble reactive phosphate (PO_4^{3-}), ammonium (NH_4^+), nitrate + nitrite ($\text{N} + \text{N}$; $\text{NO}_3^- + \text{NO}_2^-$), silicate (SiO_4) and total dissolved nitrogen and phosphorus (TDN, TDP; via in-line persulfate/UV oxidation). DOC and TDN samples (GF/F filtrate frozen in glass vials) were measured as non-purgeable organic carbon and nitrogen via acidification, sparging and high-temperature catalytic oxidation on a Shimadzu TOC-L with TMN-L attachment, ensuring that Deep Seawater Reference waters from the University of Miami Consensus Reference Materials Project measured within specifications in each run to facilitate comparison of results to those obtained by the international DOM community.

Chlorophyll *a* (Chl*a*) concentrations were measured by acetone extraction and fluorescence spectroscopy on a modified Turner 10-AU fluorometer following Welschmeyer (1994). Particulate organic carbon (POC) and nitrogen (PON) concentrations were determined via filter combustion on an Exeter Analytical CE 440 Elemental Analyzer after acid fumigation to remove particulate inorganic carbon, drying,

weighing and packing into tin capsules. TA samples were analyzed using open cell potentiometric titrations on a 166 Mettler T50 autotitrator and calibrated against a certified reference material (Dickson et al., 2007). Salinity was measured as electrical conductivity with a combination platinum ring electrode–thermistor (Metrohm 6.0451.100) on a Metrohm conductivity module using Tiamo software (v2.4). All solute and particulate samples were analyzed in the SOEST Analytical Laboratory (<http://www.soest.hawaii.edu/S-LAB/>).

To assess field and technical replicability, a separate nutrient sample was collected in situ at a subset of 15 locations and filtered immediately through a polyethersulfone 0.45 μm groundwater cartridge filter (AquaPrep 600, Pall Life Sciences, Ann Arbor, MI, USA). Samples were stored refrigerated in 250 mL polyethylene bottles for 1 month and analyzed for salinity and by flow injection autoanalyzer in parallel with the primary samples. The replicated samples were representative of the range of biogeochemical zones, spanning 75% of the lognormal data range for each parameter. Linear models of \log_{10} -transformed data collected by the two methods demonstrated strong congruency. The two methods were highly correlated ($r > 0.98$ for TDN, TDP, PO_4^{3-} , $\text{N} + \text{N}$, SiO_4 , Salinity and $r = 0.85$ for NH_4^+). In addition, both least-squares and orthogonal (Model II or reduced major axis) regression model slopes for all 7 parameters ($p < 0.001$) were not significantly different from 1 (95% confidence intervals bracketed 1). Intercepts were nearly all non-significant (intercept $p > 0.25$, except TDP $p = 0.0027$), indicating no offset between the two sample sets; when intercepts were constrained to zero, slopes remained not significantly different from 1. This analysis indicates that measurements of standard solutes were robust to minor variation in sample collection and storage as well as field variation in sampling; the primary samples were used in all subsequent analyses.

Dissolved organic N and P (DON, DOP) were calculated as the difference between TDN, TDP and inorganic species of N and P: $\text{DOP} = \text{TDP} - \text{PO}_4^{3-}$ and $\text{DON} = \text{TDN} - \text{N} + \text{N} - \text{NH}_4^+$. TDN was measured using two separate methods: via high temperature catalytic oxidation (HTCO) and subsequent ozonation chemiluminescence of 0.7 μm filtrate (GF/F) on a Shimadzu TMN-L and via persulfate alkaline oxidation and subsequent colorimetric cadmium reduction of 0.2 μm filtrate (Sterivex) on a Seal Analytical AA3HR (described above). The two methods yielded highly correlated measures of TDN ($r = 0.97$, $n = 46$) but the HTCO method yielded consistently lower estimates of TDN (Model II lognormal regression slope of 0.85 with 95% confidence interval of 0.79 to 0.91). Estimates of DON derived from the two TDN measurements did not covary and were not significantly related to $\text{N} + \text{N}$ or DOC ($p > 0.05$). When $\text{N} + \text{N}$ concentrations exceeded $40 \mu\text{mol L}^{-1}$ estimates of DON from HTCO were negative; for all subsequent analyses, Seal autoanalyzer TDN measurements were used to maintain methodological consistency with other N and P measures.

2.4. Radon activity measurements

Coastal radon activities were measured using a RAD AQUA closed air loop continuous equilibrium exchanger accessory for the RAD7 radon detector (Durrige Inc., Billerica, MA). The system was mounted on a small boat hand-pulled along the shoreline and in perpendicular transects. The system was mounted on a small boat and hand-pulled along pre-determined GPS transects. Coastal springs and diffuse seepage was identified by moving along the shoreline and shore-perpendicular transects were used to determine the extent of significant groundwater plumes at the two focus areas. The air–water exchanger of the RAD-AQUA was fed by water using a submersible bilge pump submersed 0.2 m below the water surface. The instrument recorded radon in 5-minute integrated intervals providing a spatial resolution of 50–100 m. Radon in air values were converted to radon in water activities using temperature and salinity recorded by a YSI (V2-2) multiparameter probe (Schubert et al., 2012). It has been shown previously that the nearshore water residence time at the sampling sites is one

tidal cycle so the reported radon values are not corrected for radon decay and evasion to the atmosphere (Holleman, 2011). The radon survey covered the whole bay area but only results relevant to Black Point and Wailupe are included in this analysis.

2.5. Flow cytometry

Flow cytometry was used to measure both autofluorescent and total nucleic-acid stained cell concentrations in fixed unfiltered water samples (Nelson et al., 2011). Samples were thawed and placed in 250 μL aliquots in 96-well autosampler plates in duplicate; one of the two wells was mixed with SYBR Green I stain ($1 \times$ final concentration) within 2.5 h of analysis. Samples were analyzed on an Attune Acoustic Focusing Cytometer with Autosampler Attachment (Life Technologies, Eugene, OR, USA). Samples were run at flow speeds of $100 \mu\text{L min}^{-1}$ on standard sensitivity; 150 μL of sample was aspirated, 75 μL was counted and data was collected only from the last 50 μL (event rates were empirically determined to be steady only after 25 μL of continuous sample injection). For SYBR-stained cells a blue laser (488 nm, threshold 10,000 rfu, voltage 2300 mV) was used to excite the dye and cell counts obtained by increasing the voltage to maintain event counts of blank controls (SYBR-stained 0.2 μm filtered DIW) below 100 events s^{-1} and event counts of environmental samples below 1500 events s^{-1} . This allowed for clear gating of plankton cells as populations distinct from instrument noise in bivariate plots of sidescatter and green fluorescence (530/30 nm bandpass fluorescence; BL1 channel). For autofluorescent cells a combination threshold on Violet (405 nm) OR Blue (488 nm) laser excitation and red emission (600 nm and 640 nm longpass filters, respectively VL3 and BL3 channels, 1000 rfu, 2500 mV) was used, and size-based sidescatter gating was applied to differentiate autofluorescent photosynthetic bacterioplankton (PBact) from photosynthetic autofluorescent picoeukaryotes (PEuks). Concentrations were corrected for stain and paraformaldehyde dilution factors, and heterotrophic bacterioplankton counts (HBact) were calculated as the difference of SYBR and total autofluorescent counts. These settings were empirically tested for streamwater, coastal and open ocean heterotrophic and autofluorescent bacterioplankton from the North Pacific Subtropical Gyre down to depths of 4000 m with densities ranging from 100 to 2000 cells μL^{-1} for SYBR-stained cells and 1 to 500 cells μL^{-1} for autofluorescent cells; counts matched those derived from epifluorescent microscopy within 10% in all cases.

2.6. Fluorescent dissolved organic matter (fDOM) measurement

Analysis of fDOM was conducted on a Horiba Aqualog scanning fluorometer with 150 W Xe excitation lamp, Peltier-cooled CCD emission detector and simultaneous absorbance spectrometer. Samples were warmed to room temperature (22 °C) for 2 h while the Xe bulb warmed. Excitation–emission matrices (EEMs) were measured from each of 48 samples in a 1 cm DIW-leached and rinsed quartz cuvette (3-Q-10, Starna Cells, Atascadero, CA, USA) with 4 DIW blanks run at the start and end of the contiguous 3 h analysis period. Water was excited through a 5 nm bandpass subtractive double monochromator in declining 5 nm sequence intervals from 500 to 240 nm and emission was integrated 4 s at each step and binned in 4.65 nm intervals (8-pixel bins) from 250 to 800 nm. Scans were processed using custom scripts in Matlab (v2007b) as follows: 1) first inner filter effect correction was applied to account for the quenching of fluorescence by absorbance following the recommendations of Kothawala et al. (2013) by multiplying by the antilog of the average of absorbances at the wavelengths of excitation and emission for each fluorescence data point, 2) next EEMs were scaled to Raman units (RU) by dividing by the integrated emission range of 381 to 426 nm at an excitation of 350 nm in averaged DIW blanks (Lawaetz and Stedmon, 2009; Murphy et al., 2010) and 3) average DIW blank EEMs were subtracted from each sample.

2.7. fDOM modeling and indices

We used parallel factor analysis (PARAFAC) to derive four modeled fDOM components with the DOMFluor toolbox (v1.7; Stedmon and Bro, 2008), trimming Rayleigh and Raman scatter, testing for outliers (none were identified), deriving up to 6 PARAFAC components then using split-half validation and random initialization to determine the appropriate number of modeled components (in this case only the first 4 could be validated). We also calculated a suite of derived indices from each EEM that are commonly used to differentiate aspects of fDOM character and help interpret DOM sources. The ratio of marine-derived to terrigenous fDOM (e.g. M:C) was calculated as the ratio of fluorescence at Ex310/Em410 divided by fluorescence at Ex345/Em445 (Burdige et al., 2004). The M:C has had utility in differentiating between marine- and terrestrial-derived fDOM (Burdige et al., 2004; Helms et al., 2013). The Fluorescence index (FI; McKnight et al., 2001), calculated as the ratio of fluorescence at 470 nm to 520 nm under 370 nm excitation (Cory et al., 2010; Maie et al., 2006), expresses the ratio of terrigenous vs. autochthonous-produced humic DOM. Similarly, the fluorescent biological index (BIX), which is associated with microbially-derived and autochthonous DOM, was calculated as the ratio of fluorescence at 380 nm to 430 nm under 308 nm excitation (Huguet et al., 2009). BIX > 1 can indicate a strong signal of recent autochthonous DOM production, whereas those < 0.7 reflect older autochthonous DOM (Huguet et al., 2009). Lastly, the fluorescent humification index (HIX), often used to estimate the extent of DOM diagenesis or maturation in soils, was calculated as the integrated fluorescence from 434 to 480 nm divided by the integrated fluorescence from 300 to 346 nm under 254 nm excitation (Zsolnay et al., 1999). High HIX values (> 10) indicate aromatic DOM (potentially from terrestrial or marine humic acids) whereas low values (< 4) reflect more autochthonous origin (Birdwell and Engel, 2010). Lastly, we used the absorbance spectra to calculate specific ultraviolet absorbance (SUVA₂₅₄) by dividing the linear absorbance (m⁻¹) by DOC (mg L⁻¹) (Weishaar et al., 2003).

2.8. Statistical analyses

All nutrient, organic, carbonate, fDOM indices and flow cytometry parameters were log₁₀-transformed to better approximate a gaussian (normal) distribution before statistical analysis; raw fDOM values were normally distributed and were not transformed for statistical analysis. Hierarchical clustering (Ward's minimum variance method) was used to group samples according to similarity in multiple biogeochemical parameters as a way to define clusters of samples with similar properties. Each parameter was first standardized (by subtracting the column mean and dividing by the column standard deviation) to avoid weighting clusters by absolute measurement values. To conservatively define groups of samples according to relative proportion of SGD influence based on inorganic chemical composition, samples were initially clustered by the full suite of 7 standard inorganic solute measurements made (PO₄³⁻, N + N, NH₄⁺, SiO₄, Salinity, TA and Rn). This clustering approach differentiated samples into spatially-distributed "biogeochemical provinces" interpreted as SGD Springs, Transition SGD mixing Zones, Diffuse SGD Zones and Ambient Reef waters (detailed further in the Results section). Analysis of variance (ANOVA) was then used to test if mean values of organic parameters differed among the inorganic biogeochemical provinces and sites, with Tukey and Dunnett's post hoc tests used to assess pairwise differences among groups at $\alpha = 0.05$. Chi-square tests were used to assess similarity in cluster assignment of samples using different suites of organic variables. Pearson correlation and linear regression models (least squares and orthogonal/reduced major axis/Model II approaches) were used to assess covariance among variables.

3. Results

3.1. Distributions of dissolved inorganic solutes and delineation of groundwater influence

At each site SGD sources and dispersal patterns were clearly visualized by contour mapping of conservative inorganic solute tracer concentrations in surface samples at low tide (Fig. 2a–f). Concentration gradients were consistent with rapid dilution within 200 m of the source springs at each site. Contours of the fDOM humification index (HIX) closely tracked these conservative solute gradients across the reef platform (Fig. 2g, h), and HIX was highly correlated with salinity

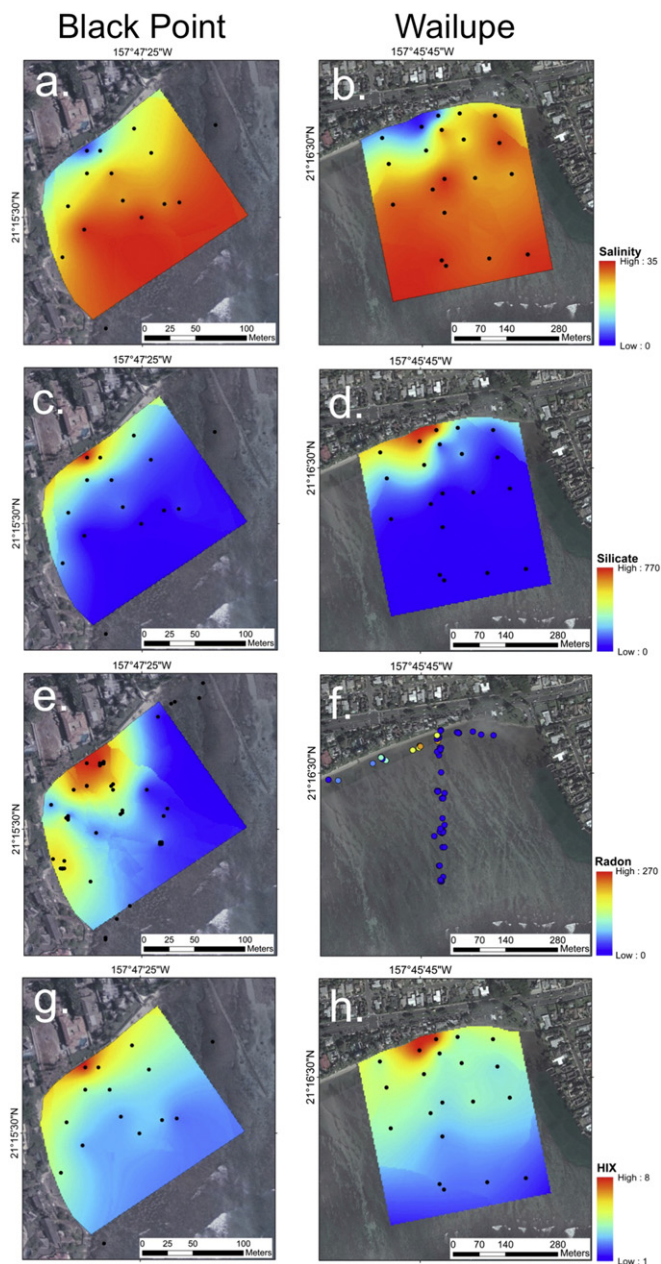


Fig. 2. Fluorescent dissolved organic matter (fDOM) in the spatial context of submarine groundwater discharge (SGD) in Maunalua Bay. Contour plots of conservative solutes and fDOM solutes at Black Point (a, c, e, g) and Wailupe (b, d, f, h) 28–29 May 2014, including salinity (a, b), silicate concentrations (c, d) ($\log_{10} \mu\text{mol L}^{-1}$), radon concentrations (e, f) (dpm L^{-1}) and the fDOM humification index (g, h) (HIX). Contour gridding and interpolation was done with the kriging function (spherical semivariogram model) in ArcGIS 10.3 Spatial Analyst. All contour plots were generated from samples collected at low tide.

and silicate consistently at both sites ($r > 0.75$; Fig. S2), demonstrating that fDOM parameters tracked salinity.

Hierarchical clustering of samples according to the suite of 7 standard inorganic solute measurements (SiO_4 , Salinity, Rn, PO_4^{3-} , N + N, NH_4^+ and TA) separated samples into six distinct groups, which we refer to subsequently as “biogeochemical provinces” because of their spatial differentiation (Fig. 3a). Groundwater springs at Wailupe and Black Point were distinct (BP Spring and WL Spring Provinces), areas of significant SGD mixing at Wailupe and Black Point were distinct

(BP Transition Zone and WL Transition Zone Provinces), while Diffuse SGD Zones and Ambient Reef provinces did not differ between sites (Fig. 3b, c). Fig. 3d, e provides a conceptual spatial schematic of the biogeochemical provinces defined in Fig. 3a that are referenced throughout this study (e.g. Spring, Transition Zone, Diffuse Zone and Ambient Reef).

At the Springs, silicate concentrations were $> 500 \mu\text{mol L}^{-1}$, salinities < 10 and radon activities $> 150 \text{ dpm L}^{-1}$ while Ambient Reef waters had silicate concentrations of $< 5 \mu\text{mol L}^{-1}$, salinities near 30 and radon activities of $< 20 \text{ dpm L}^{-1}$; transition and diffuse zones exhibited

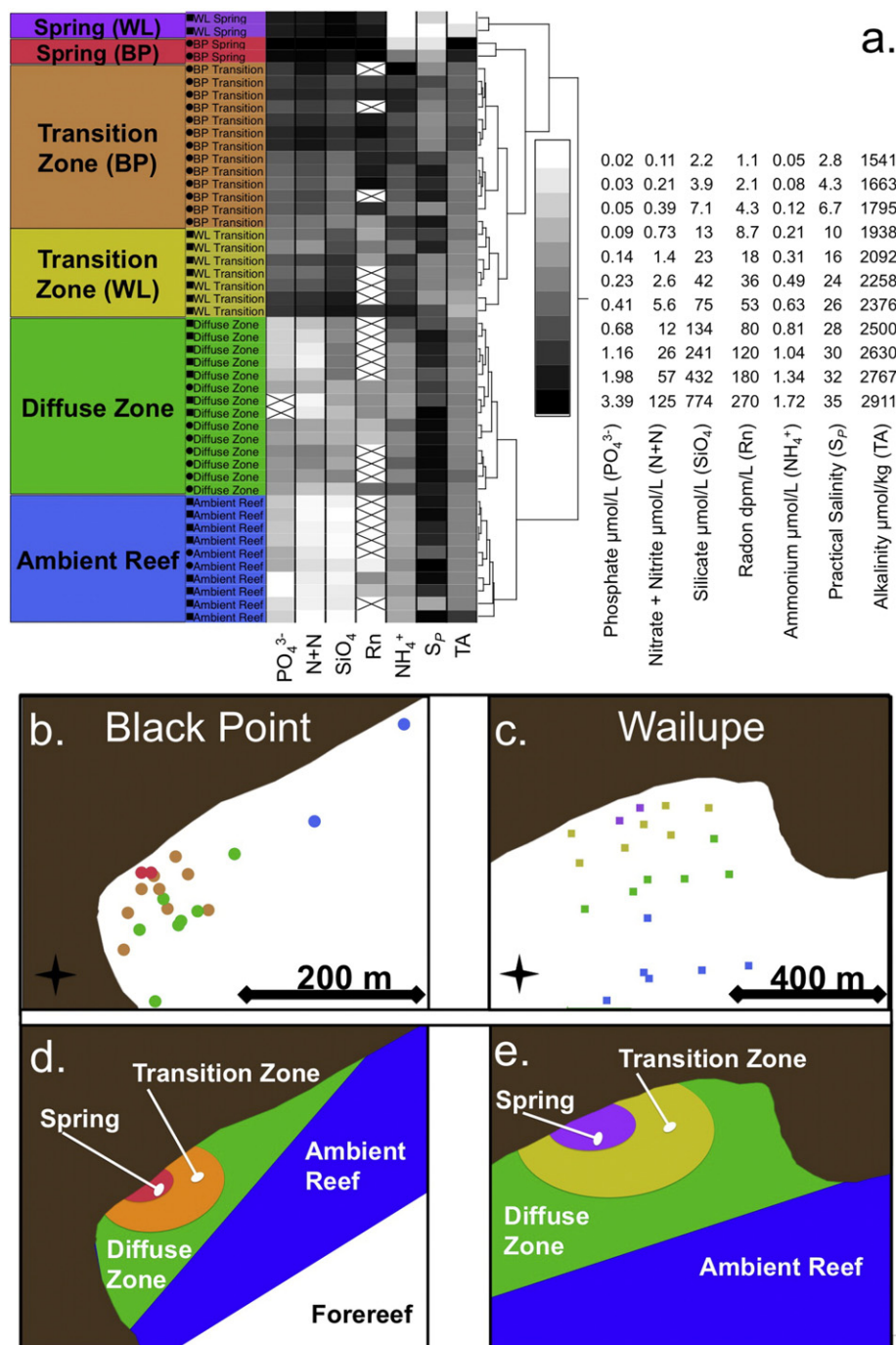


Fig. 3. Hierarchical clustering of samples into biogeochemical provinces according to inorganic solute concentrations. Panel a is a hierarchical clustering dendrogram grouping samples according to similarity in \log_{10} concentrations of 7 inorganic solutes (shown in heat map with legends at right; X indicates no data). The tips of the dendrogram are colored to match the dendrogram clusters and define biogeochemical provinces by sets of samples with similar chemistry. WL refers to Wailupe and BP refers to Black Point. Panels b and c illustrate the spatial extent of each biogeochemical province by mapping the sample points color-coded by dendrogram clusters — defined with large colored boxes in panel a — at Black Point and Wailupe, respectively. Panels d and e provide a conceptual illustration of the spatial arrangement of biogeochemical provinces.

characteristic intermediate silicate concentrations and did not differ significantly from Ambient Reef sources in salinity or radon (Table 1, Fig. S3). Sites did not differ significantly in any of the inorganic tracer solutes except that Transition Zone waters had more radon at Black Point (mean 148 dpm L⁻¹) than at Wailupe (mean 43 dpm L⁻¹; Fig. S3). Springs at both sites were significantly higher in N + N (>50 μmol L⁻¹) and PO₄³⁻ (>1.5 μmol L⁻¹) than any other samples; nearby Transition Zone samples remained significantly higher (>5×) than adjacent Diffuse Zone and Ambient Reef waters that did not differ significantly from each other (<1.5 μmol L⁻¹ N + N and <0.15 μmol L⁻¹ PO₄³⁻; Fig. S4). In contrast, NH₄⁺ concentrations were depleted in Springs (near limits of detection) relative to the adjacent Transition Zone and Diffuse Zone waters, both of which were strikingly enriched in NH₄⁺ (mean 0.9 μmol L⁻¹) above Ambient Reef samples (mean 0.3 μmol L⁻¹; Table 1 and Fig. S4). TA in the groundwater Springs differed markedly between the two sites, being significantly elevated at Black Point (mean 2826 μmol kg⁻¹) and significantly depleted at Wailupe (mean 1616 μmol kg⁻¹) relative to all other biogeochemical provinces at both sites (which did not differ significantly; mean concentrations 2250 μmol kg⁻¹; Table 1 and Fig. S4).

3.2. Distributions of particulate and dissolved organics

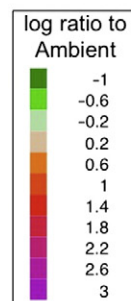
Hierarchical clustering of samples according to a suite of 9 measured dissolved and particulate organic matter concentrations and ratios (Chl *a*, Picoeukaryotic phytoplankton, autotrophic bacterioplankton, heterotrophic bacterioplankton, DOC, DON, DOP, DOC:N and TN:TP) yielded 6 distinct groups (Fig. 4a) with spatial distributions of sample types

consistent with SGD gradients (Fig. 4b, c). Group assignment of samples by clustering on inorganic solutes (Fig. 3a) and organic matter (Fig. 4a) was highly congruent (Contingency R² = 0.63, Pearson Chi-square 0.96 and *p* < 0.0001 for Low Tide samples), with 75% of the samples assigned to identical groups (Fig. 4a). Spring samples were all assigned perfectly, but Black Point samples were more homogenous spatially in terms of organic matter than observed with inorganic solutes and did not separate clearly among Transition Zone, Diffuse Zone and Ambient Reef types, potentially indicating a more extensive influence of SGD on the reef organic field (Fig. 4b). Wailupe spatial patterning of organic matter was consistent with inorganic solutes (Fig. 4c).

DOC was significantly depleted in both Springs relative to the surrounding waters (mean 85 μmol L⁻¹); concentrations in Wailupe Springs (mean 20 μmol L⁻¹) were more than twice as low as those in Black Point Springs (mean 47 μmol L⁻¹; Table 1 and Fig. S5). The two Springs had very different DON concentrations, both significantly different from the surrounding waters (mean 6.5 μmol L⁻¹), with Black Point highly enriched (mean 34 μmol L⁻¹) and Wailupe significantly depleted (mean 1.4 μmol L⁻¹). Dissolved organic phosphorus was unresolvable in Springs and near detection limits in Transition Zone regions, and did not differ among Diffuse Zones and Ambient Reef waters (mean 0.3 μmol L⁻¹). Particulate organic concentrations (POC, PON and chl *a*; Fig. S6) and flow cytometry (Picoeukaryotic phytoplankton, Autotrophic and Heterotrophic bacterioplankton; Fig. S7) pairwise differences among biogeochemical provinces were mostly non-significant due to high variance, but overall exhibited trends of particulate depletion in Springs and plankton enrichment in the surrounding Transition Zone waters (Figs. S6, S7).

Table 1
Mean values of each parameter in each of the biogeochemical provinces shaded according to magnitude of significant differences among regions. Rows are parameters, columns are biogeochemical provinces, and values are geometric means. Shaded cells are significantly different from the Ambient Reef (WL) province (denoted at the top by *; Dunnett's post hoc test), with color and intensity scaled by mean log-ratio relative to Ambient Reef waters (legend at left). POC, PON and DOP are excluded due to a lack of data to properly test each province.

	Wailupe				Black Point			
	Spring	Transition	Diffuse	Reef*	Reef	Diffuse	Transition	Spring
Practical salinity	4.2	24.4	30.4	28.8	30.5	32.6	25.5	7.1
SiO ₄ (μmol L ⁻¹)	668.5	225.2	32.2	2.8	3.2	16.6	106.8	626.9
Rn (dpm L ⁻¹)	160.4	30.4	23.7	5.6	1.7	14.2	127.2	269.7
N+N (μmol L ⁻¹)	61.63	8.50	0.24	0.14	0.23	1.16	21.15	114.16
PO ₄ ³⁻ (μmol L ⁻¹)	1.89	0.49	0.05	0.04	0.10	0.15	0.68	3.09
NH ₄ ⁺ (μmol L ⁻¹)	0.05	0.89	0.43	0.26	0.34	0.52	0.94	0.22
TA (μmol kg ⁻¹)	1614	2143	2234	2280	2238	2263	2362	2824
DOC (μmol L ⁻¹)	20.0	70.8	91.4	83.7	77.3	88.3	88.5	45.6
DON (μmol L ⁻¹)	1.4	5.0	6.8	5.7	6.1	6.6	6.6	33.6
Chl <i>a</i> (μg L ⁻¹)	0.06	0.29	0.12	0.08	0.07	0.09	0.14	0.03
HBact (cells mL ⁻¹)	4.5 × 10 ⁵	2.3 × 10 ⁵	5.0 × 10 ⁵	3.2 × 10 ⁵	3.7 × 10 ⁵	2.3 × 10 ⁵	2.2 × 10 ⁵	1.0 × 10 ⁵
PBact (cells mL ⁻¹)	1.6 × 10 ³	7.2 × 10 ³	1.8 × 10 ³	4.0 × 10 ³	1.8 × 10 ³	1.9 × 10 ³	1.4 × 10 ³	7.2 × 10 ²
PEuks (cells mL ⁻¹)	7.7 × 10 ³	9.2 × 10 ⁴	6.6 × 10 ³	6.0 × 10 ³	4.9 × 10 ³	5.2 × 10 ³	6.8 × 10 ³	5.4 × 10 ³
fDOM: A	0.028	0.061	0.056	0.025	0.029	0.037	0.052	0.075
fDOM: M	0.036	0.073	0.065	0.029	0.034	0.043	0.062	0.091
fDOM: C	0.006	0.018	0.018	0.007	0.009	0.011	0.015	0.017
fDOM: T	0.008	0.026	0.026	0.016	0.017	0.021	0.027	0.023
SUVA ₂₅₄	0.95	0.87	0.82	0.65	0.98	0.72	0.88	1.44
M:C	1.25	1.11	1.05	1.02	1.01	1.03	1.07	1.20
FI	1.82	1.72	1.73	1.73	1.79	1.75	1.75	1.76
BIX	0.83	0.79	0.82	0.80	0.84	0.83	0.82	0.85
HIX	7.78	4.28	3.60	2.35	2.74	3.00	3.47	6.98



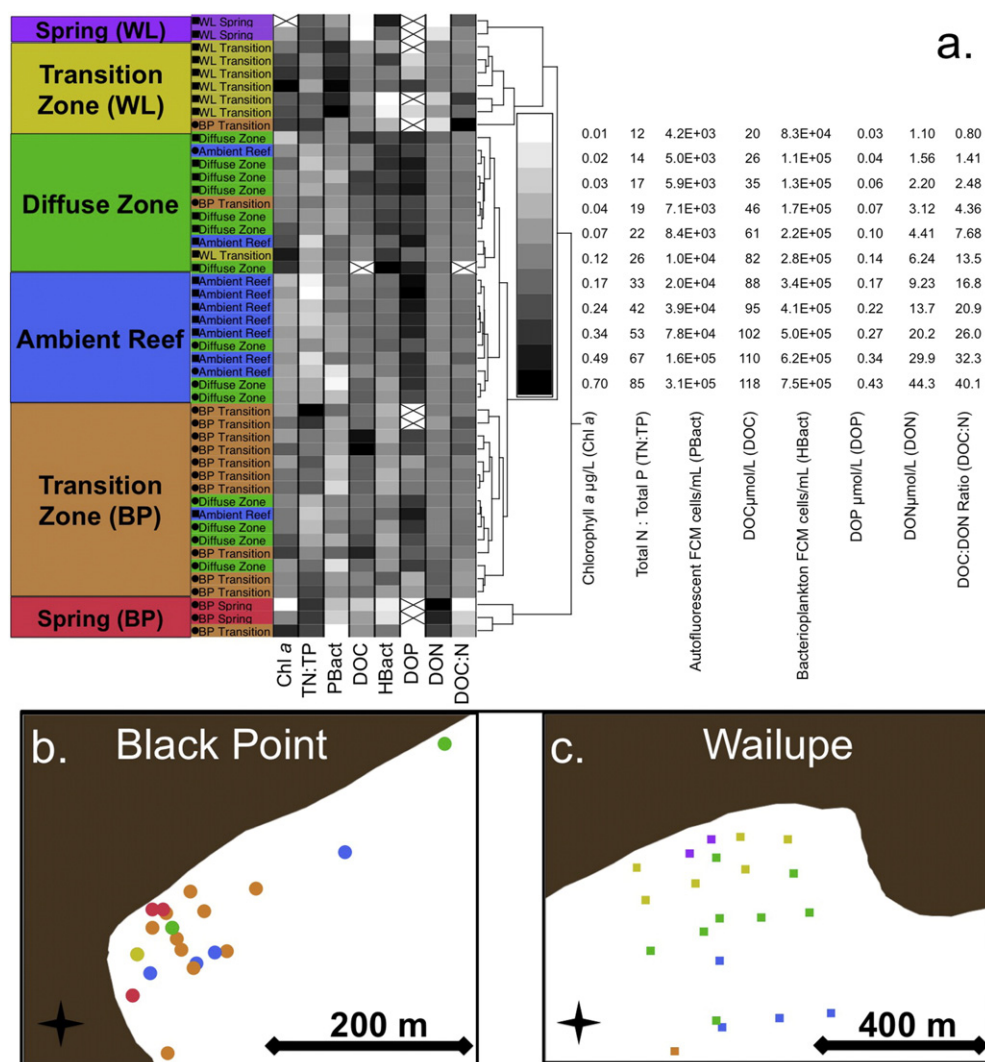


Fig. 4. Hierarchical clustering of samples according to particulate and dissolved organic matter concentrations. Panel a is a hierarchical clustering dendrogram grouping samples (tips colored according to biogeochemical provinces delineated in Fig. 3) according to similarity in \log_{10} concentrations of 8 organic measurements (shown in heat map with legends at right; X indicates no data). Panels b and c define the spatial extent of organic provinces by mapping the sample points color-coded by dendrogram clusters — defined with large colored boxes in panel a — at Black Point and Wailupe, respectively.

3.3. fDOM characteristics and distributions

The PARAFAC modeling validated 4 fluorescence components that co-varied with fluorescence regions widely identified from marine systems (regions: A — humic-like UV excitation; M — visible, blue-shifted, marine humic-like; C — visible excitation, humic-like; and T — aromatic amino protein-like; Coble, 1996) both in terms of spectral characteristics (Fig. S8) and in terms of standardized distributions among variables within this dataset (Fig. S8e). In addition, the spectral loadings of our PARAFAC components (Fig. S8a–d) matched PARAFAC components found in marine systems in various recent reviews: Component 1 ($Em(2^\circ)/Ex$: 260(375) nm/375 nm) is consistent with component C1 from Jørgensen et al. (2011) and component C2 from Ishii and Boyer (2012). Our Component 2 ($Em(2^\circ)/Ex$: <250(325) nm/400–480 nm) corresponds to component C4 from Jørgensen et al. (2011) and component C3 from Ishii and Boyer (2012). Component 3 ($Em/Ex(2^\circ)$: 300–380 nm/510(480 nm)) corresponds to component C4 in Kowalczyk et al. (2009). Component 4 ($Ex/Em(2^\circ)$: 260 nm/330(510 nm)) corresponds to component C2 in Jørgensen et al. (2011).

Each of the four PARAFAC components differed significantly among the biogeochemical provinces (ANOVA $p < 0.0001$). At Black Point both Spring and Transition Zone provinces were enriched

relative to Diffuse Zone and Ambient Reef waters for all components, indicating that total fDOM was elevated in the groundwater. In contrast, Wailupe transition and diffuse zones were enriched relative to both Spring and Ambient Reef waters (Fig. 5), consistent with the idea of production of fDOM in the SGD-influenced reef waters of Wailupe. Notably, at Black Point, although fDOM decreased from Spring to Ambient Reef waters, DOC exhibited some enrichment in the transition and diffuse zones, suggesting that autochthonous production of non-fluorescent DOM may have occurred in the diffuse zones.

Within any of the four biogeochemical provinces there were clear site differences in fDOM quantity: Black Point Spring samples were enriched in all four components relative to Wailupe Springs while the reverse was true in Diffuse Zone samples, with Wailupe enriched for components A, M and C (Fig. 5), again consistent with the idea of production of fDOM in the SGD-influenced reef waters of Wailupe.

The four ratio-based fDOM indices exhibited very different patterns within sites, emphasizing that each index is assessing a different aspect of the character of fDOM (Fig. 6). In SGD Springs, the humification index, HIX, was more than double (>7) Ambient Reef values (<3) at both sites (Table 1). HIX was highly correlated with salinity and silicate

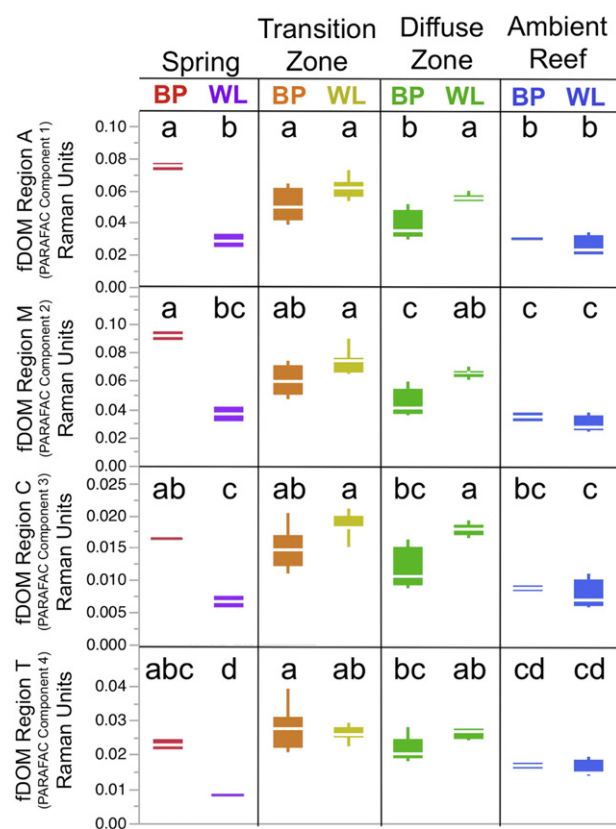


Fig. 5. Comparison of fDOM PARAFAC components among the biogeochemical provinces in each reef site. Boxes depict standard interquartile ranges with medians and are labeled at the top with letters for ANOVA Tukey post hoc tests; all ANOVA models $p < 0.0001$ and samples with different letters are significantly different at $\alpha = 0.05$.

consistently between sites ($r > 0.75$; Fig. S2) and declined continuously with distance from the Springs (Fig. 2). The M:C index covaried with HIX ($r = 0.83$) and was also significantly enriched in Springs and in Transition Zone waters relative to the Diffuse Zone and Ambient Reef waters. Relative to ambient waters, the Wailupe Spring had a significantly higher fluorescence index (FI) and $SUVA_{254}$ was significantly greater in the Black Point Spring. BIX ranged from 0.76 to 0.86 across both sites, and was generally elevated in Black Point relative to Wailupe, but did not differ significantly among water types. Indices did not differ between sites within a given biogeochemical province (Fig. 6).

Hierarchical clustering of samples according to a suite of 9 fDOM-derived parameters (4 PARAFAC components, 4 fDOM indices and $SUVA_{254}$) separated samples into 6 groups (Fig. 7a) with spatial distributions of sample types consistent with SGD gradients (Fig. 7b, c). Group assignment of samples by fDOM characteristics was generally congruent with clustering by inorganic solutes (Fig. 3) and organic matter (Fig. 7; Contingency $R^2 = 0.52$ and 0.50 , respectively, Pearson Chi-square 93 and 78, respectively and $p < 0.0001$ for Low Tide samples), with 70% of the samples assigned to identical groups. As with the organic matter clustering, Spring samples were all assigned perfectly, but at both sites the other biogeochemical provinces were less clearly differentiated spatially in terms of fDOM than observed with inorganic solutes. Notably, both Transition Zone and Diffuse Zone samples appeared to be different in fDOM parameters between Wailupe and Black Point (Fig. 7a), potentially indicating a more extensive influence of SGD on the reef fDOM field. The two SGD springs (and the two diffuse zones) may be differentiated according to their fDOM amount (i.e. fluorescence intensities of fluorophores) (Fig. 5) but cannot be clearly discriminated by fluorophore ratio indices (Fig. 6).

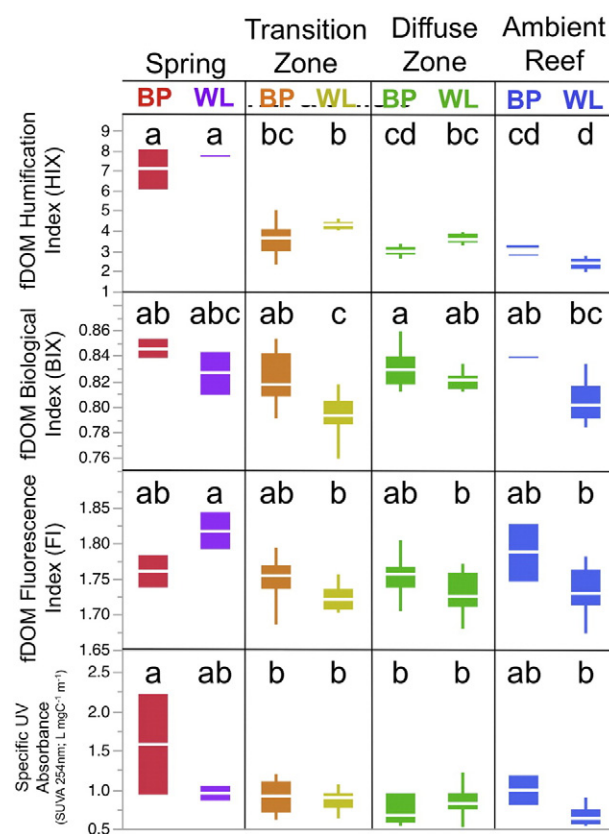


Fig. 6. Comparison of fDOM indices among the biogeochemical provinces in each reef site. Boxes depict standard interquartile ranges with medians and are labeled at the top with letters for ANOVA Tukey post hoc tests; all ANOVA models $p < 0.01$ and samples with different letters are significantly different at $\alpha = 0.05$.

4. Discussion

4.1. Biogeochemical characteristics of groundwater entering Maunalua Bay

Groundwater discharging from springs in Maunalua Bay showed some consistencies and differences between the Black Point and Wailupe sites. Both sites released groundwater with biogeochemical profiles consistent with previous studies of SGD in coral reefs (Swarzenski et al., 2013), including low salinities and elevated concentrations of radon and silicate, elevated PO_4^{3-} and $N + N$, depleted NH_4^+ concentrations and depleted DOC, POC, chl *a* and phytoplankton cells (Table 1, Figs. 2–4 and S3–S7). However, some measurements were strongly and significantly different between the two Springs. First, the Wailupe Springs were significantly depleted in TA and DON relative to the adjacent waters whereas the Black Point TA and DON were significantly greater than the adjacent waters, suggesting a fundamentally different hydrological origin (Figs. S4, S5). Second, while both Springs were depleted in DOC relative to the adjacent waters, the Wailupe site had nearly half the DOC concentrations of the Black Point site (Fig. S5), yet Black Point Springs were strongly depleted in bacterioplankton, nearly 4 times less than Wailupe Springs or the surrounding ocean (Fig. S7). Aside from the unexpectedly high concentrations of bacterioplankton in the Wailupe Springs, these patterns suggest that groundwater flow paths at these two sites are very different, potentially capturing differences in land-use and geology in these two parts of the watershed. Black Point has a higher density of on-site sewage disposal (septic and cesspool) systems (Whittier and El-Kadi, 2009), but we do not have evidence that the high nutrient or fDOM levels are due to these potential sources. The difference in radon concentrations between the springs (Table 1) suggest that groundwater at Black Point flows through rocks generating more radon (i.e., more enriched in U

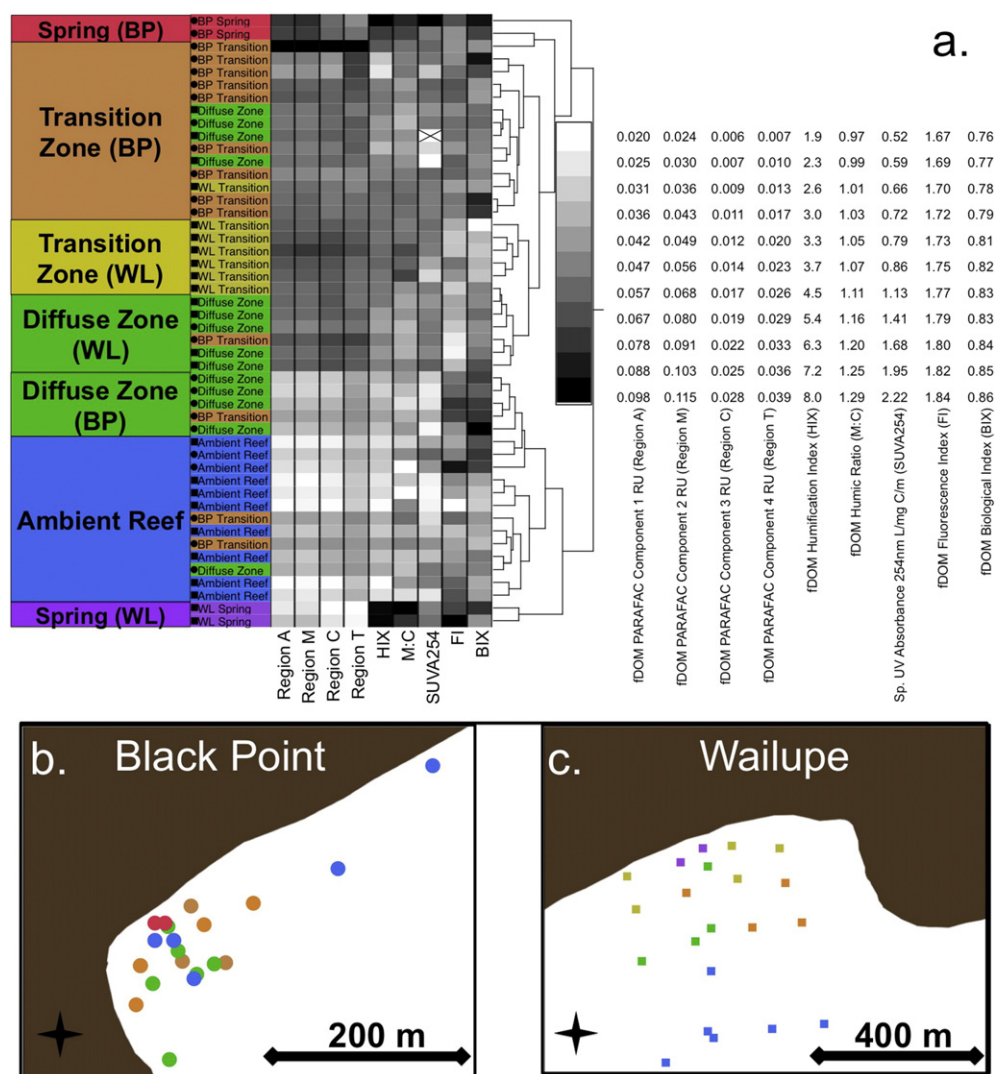


Fig. 7. Hierarchical clustering of samples according to fDOM spectral characteristics. Panel a is a hierarchical clustering dendrogram grouping samples (tips colored according to biogeochemical provinces delineated in Fig. 3) according to similarity in fDOM PARAFAC components and ratio-based indices (shown in heat map with legends at right; X indicates no data). Panels b and c define the spatial extent of fDOM character by mapping the sample points color-coded by dendrogram clusters – defined with large colored boxes in panel a – at Black Point and Wailupe, respectively.

and Ra) than the rocks and sediments at Wailupe, indicating differences in the geologic make-up of the aquifer. Land-use, including density of septic systems, presence of historic agricultural sites, etc. is a likely cause for differences in nutrient and organic matter levels.

4.2. fDOM characteristics of groundwater entering Maunalua Bay

Across sites, SGD was significantly enriched in aromatic/humic components (e.g., Regions A and M, HIX, and M:C) and had higher specific ultraviolet absorbance (Table 1). The Black Point Springs had significantly more of all 4 fDOM components than the Wailupe Springs and were enriched in all components relative to the Ambient Reef waters (Fig. 5); the Wailupe Springs had fDOM quantities identical to Ambient Reef waters for all four components. The lack of significant differences in fDOM indices between these two sites within any given biogeochemical province (Fig. 6) suggests that SGD fDOM molecular composition was similar. However, groundwater DOC concentrations overall were significantly lower than the overlying reef, and when combined with elevated fDOM (at least at Black Point) and significantly higher ratios of humic compounds (HIX Index, Figs. 2 and 6) our data indicate that a greater proportion of the DOC in the groundwater is fluorescent. Indeed, ratios between any of the four PARAFAC components and DOC concentrations,

a proxy for specific fDOM fluorescence, were significantly enriched in both Springs relative to the adjacent waters (ANOVA with Tukey post hoc $p < 0.0001$), indicating that groundwater DOC has a much higher fluorescence than marine DOC. Although both overall fDOM and DOC concentrations were significantly higher in the Black Point site (Figs. 5 and S5), ratios of fDOM components to DOC did not differ between sites, only between biogeochemical provinces, again emphasizing that the DOC in SGD is consistently highly fluorescent with a strong humic component (Figs. 2, 6, S2).

4.3. Dispersal and biogeochemical influence of submarine groundwater discharge

In an observational study it is difficult to separate cause from effect, and in the case of the current dataset we cannot definitively determine whether parameters that differ significantly in the transition and diffuse zones from the Ambient Reef waters are driven by dilution of SGD or stimulation of biogeochemical processes that subsequently alter the characteristics of the water. However, the vast majority of the measured parameters exhibited statistically robust gradients spatially concordant with SGD dispersal across the reef. A handful of parameters did not follow this trend, and it is likely that these represent reef-specific

production or consumption processes. Ammonium was the only inorganic solute that exhibited enrichment in the Transition Zone and Diffuse Zone provinces above both Spring and Ambient Reef endmembers, suggesting a production process (Fig. S4). Moreover, this parameter was only significantly enriched in the Transition Zone province, not in the adjacent Reef waters, possibly indicating rapid consumption and ammonification of DON, dissimilatory reduction of nitrate to ammonia (DNRA), or recycling of nitrate to ammonia through organic assimilation and remineralization. A similar pattern was observed in particulate organic matter, with the Wailupe site exhibiting enriched Chl *a* and eukaryotic phytoplankton counts suggestive of some stimulation of water column productivity by the groundwater nutrient delivery. Finally, there was consistent enrichment of fDOM components A, C and T in the Transition Zone and Diffuse Zone provinces above levels found in the Springs and Ambient Reef zones (Fig. 5). Region C has been associated with microbial production processes in marine systems and Region T is generally associated with proteinaceous material because of the similarities to pure tryptophan fluorescence (Coble et al., 2014). One interpretation of these patterns is that these components represent fDOM being produced by the reef habitat; whether that production is influenced directly or indirectly by SGD inputs or is simply a characteristic of reefs generally is not currently known. Certainly there are potential physicochemical changes in DOM across these gradients due to photodegradation, metal-ligand bonding, pH, and salinity shifts that impart changes to fDOM character (Helms et al., 2013; Osburn et al., 2013).

4.4. Recommendations for the use of fDOM to track groundwater discharge in reefs

This study shows clearly how fDOM spectral analyses can be used to differentiate water masses according to the degree of influence of SGD in two sites with very different SGD organic matter profiles, consistent with previous work conducted in coral reef environments with allochthonous DOM inputs (Tedetti et al., 2011). Based on our observations, it is clear that groundwater entering Maunalua Bay contains a significant quantity of fDOM with more than double the humification index (HIX) of the receiving Diffuse Zone and Ambient Reef waters (Fig. 6, Table 1), consistent with fDOM from sedimentary and volcanic sources in reef ecosystems (Tedetti et al., 2011). This single feature of the fDOM spectra (i.e., elevated HIX) was strongly correlated with both salinity and silicate in both sites with identical slopes, and from this simple index there is the potential to model these inorganic solute concentrations from the HIX value (Fig. S2). In addition, the groundwater sources to Black Point stood out clearly from the surrounding reef in humic fluorescence regions A and M (Fig. 5), though not at Wailupe. These differences suggest that fDOM characteristics may be able to differentiate groundwater according to land use, hydrology, or other factors, allowing the development of fDOM as a groundwater source-tracking tool in concert with other biogeochemical parameters. Future studies should consider the use of continuous sensor monitoring of coastal fDOM (our PARAFAC component C1 exhibits a secondary emission peak corresponding to the excitation–emission maxima of commercial DOM sensors) and examination of the interacting roles of photobleaching and residence time in defining the extent of fDOM distributions in coastal waters. Because fDOM samples are relatively easy to collect (filtering a few mL of water into glass vials and dark refrigerated storage), are unaffected by gas exchange and quick to analyze (the scans took less than 5 min each), fDOM may prove a cost-effective and efficient monitoring tool for mapping groundwater dispersal in reefs. Analyzing a sample EEM spectra also provides a wealth of additional ratio-based indices and values of the literature-derived identified spectral regions and our results hint that with larger datasets from more reefs fDOM may be used as cost-effective monitoring tool to identify new and promising indices to differentiate SGD within coastal waters.

Acknowledgments

The project described in this publication was supported in part by a grant/cooperative agreement from the National Oceanic and Atmospheric Administration, Projects R/SB-14PD (CEN), R/SB-13 (FIMT), R/SB-12 (MJD) and R/SB-11 (HD) sponsored by the University of Hawai'i Sea Grant College Program, School of Ocean and Earth Science and Technology, under Institutional Grant No. NA14OAR4170071 from the NOAA National Sea Grant Office, Department of Commerce (UNIHI-SEAGRANT-JC-14-29). SJG was supported in part by Cooperative Agreement Number G12AC00003 from the United States Geological Survey (USGS). NJS was supported by a NOAA Dr. Nancy Foster Scholarship. CR and KL are supported by the National Science Foundation Graduate Research Fellowship. This is HIMB contribution 1618 and SOEST contribution 9448. The funders had no role in the study design, data collection and analysis, decision to publish, or preparation of the manuscript. The contents of this publication are solely the responsibility of the authors and do not necessarily represent the official views of the USGS, NOAA, or any of their respective subagencies.

References

- Allredge, A., Carlson, C., Carpenter, R., 2013. Sources of organic carbon to coral reef flats. *Oceanography* 26, 108–113. <http://dx.doi.org/10.5670/oceanog.2013.52>.
- Azam, F., Fenchel, T., Field, J., Gray, J., Meyer-Reil, L., Thingstad, F., 1983. The ecological role of water-column microbes in the sea. *Mar. Ecol. Prog. Ser.* 10, 257–263.
- Beck, A.J., Tsukamoto, Y., Tovar-Sanchez, A., Huerta-Diaz, M., Bokuniewicz, H.J., Sañudo-Wilhelmy, S.A., 2007. Importance of geochemical transformations in determining submarine groundwater discharge-derived trace metal and nutrient fluxes. *Appl. Geochem.* 22, 477–490. <http://dx.doi.org/10.1016/j.apgeochem.2006.10.005>.
- Birdwell, J.E., Engel, A.S., 2010. Characterization of dissolved organic matter in cave and spring waters using UV–Vis absorbance and fluorescence spectroscopy. *Org. Geochem.* 41, 270–280. <http://dx.doi.org/10.1016/j.orggeochem.2009.11.002>.
- Burdige, D.J., Kline, S.W., Chen, W., 2004. Fluorescent dissolved organic matter in marine sediment pore waters. *Mar. Chem.* 89, 289–311. <http://dx.doi.org/10.1016/j.marchem.2004.02.015>.
- Burnett, W.C., Aggarwal, P.K., Aureli, A., Bokuniewicz, H., Cable, J.E., Charette, M.A., Kontar, E., Krupa, S., Kulkarni, K.M., Loveless, A., Moore, W.S., Oberdorfer, J.A., Oliveira, J., Ozyurt, N., Povinec, P., Privitera, A.M.G., Rajar, R., Ramessur, R.T., Scholten, J., Stieglitz, T., Taniguchi, M., Turner, J.V., 2006. Quantifying submarine groundwater discharge in the coastal zone via multiple methods. *Sci. Total Environ.* 367, 498–543. <http://dx.doi.org/10.1016/j.scitotenv.2006.05.009>.
- Charette, M.A., Moore, W.S., Burnett, W.C., 2008. Chapter 5. Uranium- and thorium-series nuclides as tracers of submarine groundwater discharge. In: Cochran, S.K., J.K. (Eds.), *Radioactivity in the Environment, U–Th Series Nuclides in Aquatic Systems*. Elsevier, pp. 155–191.
- Chen, W., Westerhoff, P., Leenheer, J.A., Booksh, K., 2003. Fluorescence excitation–emission matrix regional integration to quantify spectra for dissolved organic matter. *Environ. Sci. Technol.* 37, 5701–5710. <http://dx.doi.org/10.1021/es034354c>.
- Coble, P.G., 1996. Characterization of marine and terrestrial DOM in seawater using excitation–emission matrix spectroscopy. *Mar. Chem.* 51, 325–346.
- Coble, P., Lead, J., Baker, A., Reynolds, D., Spencer, R.G.M., 2014. *Aquatic Organic Matter Fluorescence*. Cambridge University Press.
- Cory, R.M., Miller, M.P., McKnight, D.M., Guerard, J.J., Miller, P.L., 2010. Effect of instrument-specific response on the analysis of fulvic acid fluorescence spectra. *Limnol. Oceanogr. Methods* 8, 67–78.
- Cyronak, T., Santos, I.R., Erler, D.V., Maher, D.T., Eyre, B.D., 2014. Drivers of pCO₂ variability in two contrasting coral reef lagoons: the influence of submarine groundwater discharge. *Glob. Biogeochem. Cycles* 28. <http://dx.doi.org/10.1002/2013GB004598> (2013GB004598).
- Dabestani, R., Ivanov, I.N., 1999. A compilation of physical, spectroscopic and photophysical properties of polycyclic aromatic hydrocarbons. *Photochem. Photobiol.* 70, 10–34. <http://dx.doi.org/10.1111/j.1751-1097.1999.tb01945.x>.
- Dalier, M.L., Knox, R.S., Smith, J.E., Napier, M., Smith, C.M., 2010. Using $\delta^{15}\text{N}$ values in algal tissue to map locations and potential sources of anthropogenic nutrient inputs on the island of Maui, Hawaii, USA. *Mar. Pollut. Bull.* 60, 655–671. <http://dx.doi.org/10.1016/j.marpolbul.2009.12.021>.
- Determann, S., Lobbes, J.M., Reuter, R., Rullkötter, J., 1998. Ultraviolet fluorescence excitation and emission spectroscopy of marine algae and bacteria. *Mar. Chem.* 62, 137–156. [http://dx.doi.org/10.1016/S0304-4203\(98\)00026-7](http://dx.doi.org/10.1016/S0304-4203(98)00026-7).
- Dickson, A.G., Sabine, C.L., Christian, J.R., et al., 2007. *Guide to Best Practices for Ocean CO₂ Measurements*.
- Dimova, N.T., Swarzenski, P.W., Dulaiova, H., Glenn, C.R., 2012. Utilizing multichannel electrical resistivity methods to examine the dynamics of the fresh water–seawater interface in two Hawaiian groundwater systems. *J. Geophys. Res. Oceans* 117, C02012. <http://dx.doi.org/10.1029/2011JC007509>.
- Dollar, S.J., Atkinson, M.J., 1992. Effects of nutrient subsidies from groundwater to nearshore marine ecosystems off the island of Hawaii. *Estuar. Coast. Shelf Sci.* 35, 409–424. [http://dx.doi.org/10.1016/S0272-7714\(05\)80036-8](http://dx.doi.org/10.1016/S0272-7714(05)80036-8).

- Fabrizius, K., 2005. Effects of terrestrial runoff on the ecology of corals and coral reefs: review and synthesis. *Mar. Pollut. Bull.* 50, 125–146.
- Ferretto, N., Tedetti, M., Guigue, C., Mounier, S., Redon, R., Goutx, M., 2014. Identification and quantification of known polycyclic aromatic hydrocarbons and pesticides in complex mixtures using fluorescence excitation–emission matrices and parallel factor analysis. *Chemosphere* 107, 344–353. <http://dx.doi.org/10.1016/j.chemosphere.2013.12.087>.
- Goñi, M.A., Gardner, I.R., 2003. Seasonal dynamics in dissolved organic carbon concentrations in a coastal water-table aquifer at the forest–marsh interface. *Aquat. Geochem.* 9, 209–232. <http://dx.doi.org/10.1023/B:AQUA.0000022955.82700.ed>.
- Hansell, D.A., Carlson, C.A., 2014. *Biogeochemistry of Marine Dissolved Organic Matter*. 2nd ed. Elsevier.
- Helms, J.R., Stubbins, A., Perdue, E.M., Green, N.W., Chen, H., Mopper, K., 2013. Photochemical bleaching of oceanic dissolved organic matter and its effect on absorption spectral slope and fluorescence. *Mar. Chem.* 155, 81–91. <http://dx.doi.org/10.1016/j.marchem.2013.05.015>.
- Holleman, K., 2011. *Comparison of Submarine Groundwater-derived Nutrients From Leeward Flanks of the Islands of Oahu and Hawaii MS Thesis*, Dept. of Geology and Geophysics. Univ. of Hawaii at Mānoa, Honolulu, HI, USA.
- Huang, W.-J., Wang, Y., Cai, W.-J., 2012. Assessment of sample storage techniques for total alkalinity and dissolved inorganic carbon in seawater. *Limnol. Oceanogr. Methods* 10, 711–717. <http://dx.doi.org/10.4319/lom.2012.10.711>.
- Huguet, A., Vacher, L., Relexans, S., Saubusse, S., Froidefond, J.M., Parlanti, E., 2009. Properties of fluorescent dissolved organic matter in the Gironde estuary. *Org. Geochem.* 40, 706–719. <http://dx.doi.org/10.1016/j.orggeochem.2009.03.002>.
- Ishii, S.K.L., Boyer, T.H., 2012. Behavior of reoccurring PARAFAC components in fluorescent dissolved organic matter in natural and engineered systems: a critical review. *Environ. Sci. Technol.* 46, 2006–2017. <http://dx.doi.org/10.1021/es2043504>.
- Johnson, E.E., Wiegner, T.N., 2013. Surface water metabolism potential in groundwater-fed coastal waters of Hawaii Island, USA. *Estuar. Coasts* 37, 712–723. <http://dx.doi.org/10.1007/s12237-013-9708-y>.
- Johnson, A.G., Glenn, C.R., Burnett, W.C., Peterson, R.N., Lucey, P.G., 2008. Aerial infrared imaging reveals large nutrient-rich groundwater inputs to the ocean. *Geophys. Res. Lett.* 35, L15606. <http://dx.doi.org/10.1029/2008GL034574>.
- Jørgensen, L., Stedmon, C.A., Kragh, T., Markager, S., Middelboe, M., Søndergaard, M., 2011. Global trends in the fluorescence characteristics and distribution of marine dissolved organic matter. *Mar. Chem.* 126, 139–148. <http://dx.doi.org/10.1016/j.marchem.2011.05.002>.
- Kim, G., Kim, J.-S., Hwang, D.-W., 2011. Submarine groundwater discharge from oceanic islands standing in oligotrophic oceans: implications for global biological production and organic carbon fluxes. *Limnol. Oceanogr.* 56, 673–682. <http://dx.doi.org/10.4319/lo.2011.56.2.0673>.
- Kim, T.-H., Waska, H., Kwon, E., Suryaputra, I.G.N., Kim, G., 2012. Production, degradation, and flux of dissolved organic matter in the subterranean estuary of a large tidal flat. *Mar. Chem.* 142–144, 1–10. <http://dx.doi.org/10.1016/j.marchem.2012.08.002>.
- Knee, K.L., Gossett, R., Boehm, A.B., Paytan, A., 2010. Caffeine and agricultural pesticide concentrations in surface water and groundwater on the north shore of Kauai (Hawaii, USA). *Mar. Pollut. Bull.* 60, 1376–1382. <http://dx.doi.org/10.1016/j.marpolbul.2010.04.019>.
- Kothawala, D.N., Murphy, K.R., Stedmon, C.A., Weyhenmeyer, G.A., Tranvik, L.J., 2013. Inner filter correction of dissolved organic matter fluorescence. *Limnol. Oceanogr. Methods* 11, 616–630. <http://dx.doi.org/10.4319/lom.2013.11.616>.
- Kowalczyk, P., Durako, M.J., Young, H., Kahn, A.E., Cooper, W.J., Gonsior, M., 2009. Characterization of dissolved organic matter fluorescence in the South Atlantic Bight with use of PARAFAC model: interannual variability. *Mar. Chem.* 113, 182–196. <http://dx.doi.org/10.1016/j.marchem.2009.01.015>.
- Lapointe, B.E., 1997. Nutrient thresholds for bottom-up control of macroalgal blooms on coral reefs in Jamaica and southeast Florida. *Limnol. Oceanogr.* 42, 1119–1131. http://dx.doi.org/10.4319/lo.1997.42.5_part_2.1119.
- Lawaetz, A.J., Stedmon, C.A., 2009. Fluorescence intensity calibration using the Raman scatter peak of water. *Appl. Spectrosc.* 63, 936–940.
- Lee, Y.-W., Kim, G., Lim, W.-A., Hwang, D.-W., 2010. A relationship between submarine groundwater borne nutrients traced by Ra isotopes and the intensity of dinoflagellate red-tides occurring in the southern sea of Korea. *Limnol. Oceanogr.* 55, 1–10. <http://dx.doi.org/10.4319/lo.2010.55.1.0001>.
- Maie, N., Parish, K.J., Watanabe, A., Knicker, H., Benner, R., Abe, T., Kaiser, K., Jaffé, R., 2006. Chemical characteristics of dissolved organic nitrogen in an oligotrophic subtropical coastal ecosystem. *Geochim. Cosmochim. Acta* 70, 4491–4506. <http://dx.doi.org/10.1016/j.gca.2006.06.1554>.
- McCook, L.J., 1999. Macroalgae, nutrients and phase shifts on coral reefs: scientific issues and management consequences for the Great Barrier Reef. *Coral Reefs* 18, 357–367. <http://dx.doi.org/10.1007/s003380050213>.
- McKnight, D.M., Boyer, E.W., Westerhoff, P.K., Doran, P.T., Kulbe, T., Andersen, D.T., 2001. Spectrofluorometric characterization of dissolved organic matter for indication of precursor organic material and aromaticity. *Limnol. Oceanogr.* 46, 38–48.
- Moore, W.S., 2010. The effect of submarine groundwater discharge on the ocean. *Ann. Rev. Mar. Sci.* 2, 59–88. <http://dx.doi.org/10.1146/annurev-marine-120308-081019>.
- Murphy, K.R., Butler, K.D., Spencer, R.G.M., Stedmon, C.A., Boehme, J.R., Aiken, G.R., 2010. Measurement of dissolved organic matter fluorescence in aquatic environments: an interlaboratory comparison. *Environ. Sci. Technol.* 44, 9405–9412. <http://dx.doi.org/10.1021/es102362t>.
- Nelson, M.B., Coble, P.G., 2009. *Optical analysis of chromophoric dissolved organic matter. Practical Guidelines for the Analysis of Seawater*. CRC Press, p. 401.
- Nelson, C.E., Alldredge, A.L., McCliment, E.A., Amaral-Zettler, L.A., Carlson, C.A., 2011. Depleted dissolved organic carbon and distinct bacterial communities in the water column of a rapid-flushing coral reef ecosystem. *ISME J.* 5, 1374–1387. <http://dx.doi.org/10.1038/ismej.2011.12>.
- Osburn, C.L., Stedmon, C.A., Spencer, R.G.M., Stubbins, A., 2013. Linking optical and chemical properties of dissolved organic matter in natural waters. *Limnol. Oceanogr. Bull.* 22, 78–81.
- Parsons, M.L., Walsh, W.J., Settlemier, C.J., White, D.J., Ballauer, J.M., Ayotte, P.M., Osada, K.M., Carman, B., 2008. A multivariate assessment of the coral ecosystem health of two embayments on the lee of the island of Hawaii. *Mar. Pollut. Bull.* 56, 1138–1149. <http://dx.doi.org/10.1016/j.marpolbul.2008.03.004>.
- Paytan, A., Shellenbarger, G.G., Street, J.H., Gonner, M.E., Davis, K., Young, M.B., Moore, W.S., 2006. Submarine groundwater discharge: an important source of new inorganic nitrogen to coral reef ecosystems. *Limnol. Oceanogr.* 51, 343–348. <http://dx.doi.org/10.4319/lo.2006.51.1.0343>.
- Santos, I.R., Burnett, W.C., Dittmar, T., Suryaputra, I.G.N.A., Chanton, J., 2009. Tidal pumping drives nutrient and dissolved organic matter dynamics in a Gulf of Mexico subterranean estuary. *Geochim. Cosmochim. Acta* 73, 1325–1339. <http://dx.doi.org/10.1016/j.gca.2008.11.029>.
- Schubert, M., Paschke, A., Lieberman, E., Burnett, W.C., 2012. Air–water partitioning of ²²²Rn and its dependence on water temperature and salinity. *Environ. Sci. Technol.* 46, 3905–3911. <http://dx.doi.org/10.1021/es204680n>.
- Smith, J.E., Hunter, C.L., Smith, C.M., 2010. The effects of top-down versus bottom-up control on benthic coral reef community structure. *Oecologia* 163, 497–507. <http://dx.doi.org/10.1007/s00442-009-1546-z>.
- Stedmon, C.A., Bro, R., 2008. Characterizing dissolved organic matter fluorescence with parallel factor analysis: a tutorial. *Limnol. Ocean. Methods* 6, 572–579.
- Stedmon, C.A., Markager, S., 2005. Tracing the production and degradation of autochthonous fractions of dissolved organic matter by fluorescence analysis. *Limnol. Oceanogr.* 50, 1415–1426.
- Stimson, J., Larned, S.T., 2000. Nitrogen efflux from the sediments of a subtropical bay and the potential contribution to macroalgal nutrient requirements. *J. Exp. Mar. Biol. Ecol.* 252, 159–180. [http://dx.doi.org/10.1016/S0022-0981\(00\)00230-6](http://dx.doi.org/10.1016/S0022-0981(00)00230-6).
- Street, J.H., Knee, K.L., Grossman, E.E., Paytan, A., 2008. Submarine groundwater discharge and nutrient addition to the coastal zone and coral reefs of leeward Hawaii. *Mar. Chem.* 109, 355–376. <http://dx.doi.org/10.1016/j.marchem.2007.08.009>.
- Swarzenski, P.W., Dulaiova, H., Dailer, M.L., Glenn, C.R., Smith, C.G., Storlazzi, C.D., 2013. A geochemical and geophysical assessment of coastal groundwater discharge at select sites in Maui and Oahu, Hawaii. In: Wetzellhuetter, C. (Ed.), *Groundwater in the Coastal Zones of Asia-Pacific*, Coastal Research Library. Springer Netherlands, pp. 27–46.
- Tedetti, M., Cuet, P., Guigue, C., Goutx, M., 2011. Characterization of dissolved organic matter in a coral reef ecosystem subjected to anthropogenic pressures (La Réunion Island, Indian Ocean) using multi-dimensional fluorescence spectroscopy. *Sci. Total Environ.* 409, 2198–2210. <http://dx.doi.org/10.1016/j.scitotenv.2011.01.058>.
- Weishaar, J.L., Aiken, G.R., Bergamaschi, B.A., Fram, M.S., Fujii, R., Mopper, K., 2003. Evaluation of specific ultraviolet absorbance as an indicator of the chemical composition and reactivity of dissolved organic carbon. *Environ. Sci. Technol.* 37, 4702–4708. <http://dx.doi.org/10.1021/es030360x>.
- Welschmeyer, N.A., 1994. Fluorometric analysis of chlorophyll a in the presence of chlorophyll b and pheopigments. *Limnol. Oceanogr.* 39, 1985–1992. <http://dx.doi.org/10.4319/lo.1994.39.8.1985>.
- Whittier, R.B., El-Kadi, A.I., 2009. *Human and Environmental Risk Ranking of Onsite Sewage Disposal Systems*. State of Hawaii Department of Health Safe Drinking Water Branch.
- Wolanski, E., Martinez, J.A., Richmond, R.H., 2009. Quantifying the impact of watershed urbanization on a coral reef: Maunaloa Bay, Hawaii. *Estuar. Coast. Shelf Sci.* 84, 259–268. <http://dx.doi.org/10.1016/j.ecss.2009.06.029>.
- Zsolnay, A., Baigar, E., Jimenez, M., Steinweg, B., Saccomandi, F., 1999. Differentiating with fluorescence spectroscopy the sources of dissolved organic matter in soils subjected to drying. *Chemosphere* 38, 45–50. [http://dx.doi.org/10.1016/S0045-6535\(98\)00166-0](http://dx.doi.org/10.1016/S0045-6535(98)00166-0).